Lamellar phase under shear : SANS measurements

Olivier Diat, D. Roux, F. Nallet

JOURNAL DE PHYSIQUE IV
Colloque C8, supplément au Journal de Physique I, Volume 3, décembre 1993

Lamellar phase under shear: SANS measurements

O. DIAT, D. ROUX* and F. NALLET*

ESRF, BP. 220, 38043 Grenoble, France
** CNRS, Centre de Recherche Paul Pascal, 33600 Pessac, France*

ABSTRACT

The static properties of lyotropic lamellar phases have been investigated for a long time. Recently, we studied the dynamic properties and more specifically the effect of shear on these phases. Using different techniques (conoscopy, light, neutron and X-ray scattering, microscopy and rheology), the different stationary orientation states of a lamellar phase (in a quaternary mixture water-SDS-pentanol-dodecane) have been analyzed ; in this paper we describe the analysis of the oriented state of these lamellar phase at high shear rates; we consider a Gaussian distribution to define the mosaicity of this orientation where the normal of the membrane is parallel to the velocity gradient.

INTRODUCTION:

We have studied the effect of shear on lyotropic lamellar phases [1,2]. This liquid crystal phase has been extensively studied elsewhere [3-7]. This system which consists of stacked membranes (surfactant bilayers with a thickness d and a repeating distance ξ) in solvent, has a long range position order perpendicular to the layers; this crystalline nature (smectic A symmetry) has been investigated by different experimental measurements in real space (microscopy) and in Fourier space (SAXS, SANS and light scattering experiments). A lot of information on the static behavior concerning the thermodynamic stability and the elastic properties of these phases have been analyzed [8-12]. The static behavior is well known and we are here interested in the dynamic properties and more specifically in the rheological behavior.
In a first part, we present briefly the shear cell and give the orientation diagram of a defined lamellar phase under shear. In a second part, we describe the evolution of the small angle neutron scattering pattern of the same lamellar phase under shear and then analyze the orientation of the membranes under high shear rate. Then we conclude according to some other results obtained by other measurements [2].

EXPERIMENTAL

When the shear rate $\dot{\gamma}$ is not larger than the characteristic frequency of the system, the effect of shear on long range ordered phases is assumed to perturbate its space organization at large scale

[13]. Thus the aim of these investigations is to determine the different orientations of the lamellar phase for different concentrations of membranes as a function of the shear rate.

Shear cell

We have constructed two Couette shear cells, one designed for small angle neutron scattering and the other one for birefringence and light scattering measurements. They consist of two concentric cylinders where the inner one is fixed and the outer one can be turned around the central vertical axis $\vec{z}$ [15,16]. Between these two cylinders, a free annular gap of the order of 1mm is filled by the sample ; this set is closed in a temperature regulated, transparent oven to keep the sample at a controlled temperature. The main difference between the 'neutron' and the 'light' cell is the transparent parts (windows and cylinders), which are respectively in quartz and glass, for absorption reasons. All the details of these cells are given in previous papers[2,17].

Sample

The studied system is a quaternary mixture where the membrane is composed of surfactant, the Sodium Dodecyl Sulfate (SDS), the pentanol, a cosurfactant, and water and the solvent separating the membranes is Dodecane. Experimental works demonstrated that this system is stabilized by entropically induced undulation forces [14]. The phase diagram is given in previous paper [5]. The dilution process consists of adding oil+pentanol (9%) to an initial concentred lamellar phase. The characteristic distance ξ can also vary from 40 to 400 Å. Several lamellar phases in this mixture were studied ; the volume fraction of membrane were 47.6, 37.44, 27.2, 16.72 and 8.92%. For neutron scattering the water has been replaced by heavy water in order to achieve a contrast between membrane and solvent. This substitution changes only very slightly the limit in the phase diagram.

Experimental set

In the static case, SANS patterns from lamellar phases exhibit a quasi-Bragg diffraction characteristic of an ordered system. Moreover, at very small angles, it has a strong dilution enhanced signal due to concentration fluctuations [7,18]. Knowing the profile of these lamellar phases in the static case, we could analyze the variation of the scattering from these lamellar phases under shear. This profile is basically unchanged under shear.

The 'neutron' Couette cell has been installed at the Léon-Brillouin Laboratory (CEA SACLAY, FRANCE) on the PAXY line built for small angle scattering, with a 2-dimensional detector. The size of the beam is 7 mm and goes through the cell perpendicularly to the surface of the cylinders. The range of the wave vector was between 1.5 10^{-2} $Å^{-1}$ and 1.5 $10^{-1}Å^{-1}$. The geometry of these experiments allow us to obtain directly information on the orientation of the membranes in the $(\vec{z}, \vec{V})$ plane (see Fig 1). We were not successful in collecting information in the other orthogonal plan. The absorption was too large because of a thicker path.

Orientation diagram [2]

We have performed SANS experiments following an orientation diagram that we have established from visual observation of the texture of the lamellar phase, between crossed polarizers, as a function of the shear rate. We have summarized these observations and some optical measurements in figure 2. In this diagram we defined 4 distinct zones as a function of the membrane volume fraction ϕ and the shear rate $\dot{\gamma}$ and respectively called I, II, II+III and III. The regions I and III correspond to an oriented lamellar phase, with the membranes parallel to the surface of the cylinders but with a distinct difference : at low shear rate (region I), the phase has plenty defects (which correspond to some disorientations of the membrane in all directions) which move in the flow. On the other hand, at higher shear rates, these defects have almost disappeared in the flow direction. Region II corresponds to a striking orientation: indeed, under shear the lamellar phase organizes itself in an assembly of close contact multilamellar vesicles or spherulites [1]. Then, the zone 'II+III' is a coexistence region with the orientation state II and III.

In the following part we will analyze the SANS experiments on lamellar phases observed in the region III, to give an idea of the mosaicity of their orientation.

SANS measurements

Two dimensional neutron scattering patterns have been collected during experiments on the PAXY line and the figure 3 shows us the typical evolution of these patterns from one lamellar sample $\phi_{37.44}$ under shear ($\phi_{37.44}$ shows that the volume fraction of membrane in the lamellar phase is 37.44%). In region I (see Fig 3a) the scattering is strongly anisotropic. When region II is reached, the scattering becomes isotropic (see Fig 3b) (this is due to the spherulite shape) and when the shear rate is in the range of region III, the scattering becomes strongly anisotropic again (see Fig 3c). We will not consider zone II+III furthermore.

Whatever the shear rate, a main remark can be done concerning this evolution : the profile of the scattered intensity versus the module of the wave vector $\vec{q}$ is the same as the one we obtain in the static case ; in particular the position of the Bragg peak at $q_0 = 2\pi/\xi$ (where ξ is the inter-membrane distance) is always the same. Thus the structure of the lamellar phase is not affected by the shear rate during the experiments.

We have studied the anisotropy of the Bragg reflection and its relative intensity in the main directions of the wave vector $\vec{q}$, q_x, q_y and q_z. These two indications are linked to the distribution of the membranes in the $(\vec{z}, \vec{V})$ plane. To simplify the following analysis, we define 3 main orientations represented in figure 4 and respectively called Z, V, ∇V orientations which correspond to the direction of the normal to the layers in the vertical, radial and tangential direction in the Couette geometry. Remember that in the geometry of this neutron experiment, the pure orientation ∇V (radial orientation) does not contribute to scattering in the detector plane.

We defined also a contrast variable C in the $(\vec{z}, \vec{V})$ plane, calculated as follows:

$$C = \frac{I_Z(q_0) - I_V(q_0)}{I_Z(q_0) + I_V(q_0)} \qquad (1)$$

where Iz and Iv correspond to the intensity of the Bragg peak in the $\vec{z}$ and the $\vec{V}$ direction respectively.

The contrast variation for different concentrations of membranes is represented in figure 5(a/, b/, c/, d/), and summarized in a generic curve in figure 5e. Notice that for the concentred sample (see Fig 5a), we describe only the first part of the generic curve (fig 5e); this indicates that if we were able to increase the shear rate above the last shear rate value we could perhaps increase the contrast towards 1; however, since the sample is very viscous, some flow instabilities appears at a higher shear rate giving an upper shear rate limit to the experiment. On the other hand, for the dilute sample, the curves 5c and 5d describe only the last part of the generic curve; indeed, we can see on the orientation diagram that at low shear rates the widths of the region I and II are very small and there are not enough experiment points to completely describe these parts.

Analysis

According to these different curves obtained in SANS, we have determined an orientation distribution, compatible with these results.

The scattered intensity from a oriented lamellar domain at a given wave vector $\vec{q}$ can be calculated as [19]:

$$I(\vec{q}) = N\, P_{\perp}(\vec{q}_{\perp})\, P_Z(q_Z)\, S(q_Z) \qquad (2)$$

where $P_{\perp}(\vec{q_{\perp}})$ is a function which takes into account the finite spatial extension of the membrane

in the plane of the layers,

$P_z(q_z)$ is the form factor of the membrane perpendicular to the layers,

$S(q_z)$ is the structure factor of the membrane in the $\vec{z}$ direction,

and N is the number of stacked membranes in this oriented domain.

We can demonstrate that this scattered intensity, averaged with a distribution $\rho(t,f)$ to the normal of the layers becomes [annex A]:

$$\overline{I(\omega, q)} = 8\pi^2 \frac{V}{d} \frac{1}{q^2} P_z(q)\, S(q)\, \rho(\pi/2, \omega) \qquad (3)$$

where V is the scattering volume, d is the period of the smectic, ω is the angle between $\vec{q}$ and the $\vec{V}$ axes in the $(\vec{z}, \vec{V})$ plane, parallel to the plan detector and t and f are the two angles defining the normal $\vec{n}$ of the membranes in the space $(\vec{z}, \vec{V}, \vec{vv})$ (see Fig 6).

According to other experiments like conoscopy measurements [2], we can assume that the distribution of the membranes at high shear rates (region III in the orientation diagram) is centered around the ∇V orientation and that the disorientation or defects can be represented by two Gaussian distributions of the direction of $\vec{n}$ in the two orthogonal planes $(\vec{z}, \vec{V})$ and $(\vec{z}, \overrightarrow{\nabla V})$, respectively characterized by the two widths δ and Δ :

$$\rho(t,f) = \frac{1}{\sqrt{2\pi}\Delta} \exp\left(-t^2/2\Delta^2\right) \frac{1}{\sqrt{2\pi}\delta} \exp\left(-(f-\pi/2)^2/2\delta^2\right) \qquad (4)$$

We introduce the intensity $I_{iso}(q_0)$ as the intensity of theBragg peaks when the distribution $\rho(t,f)$ is isotropic and equal to $1/4\pi$; its value is determined either by the intensity of the Bragg ring in the region II (isotropic orientation of the membrane due to the spherulite shape) or in the $\vec{z}$ direction at the beginning of zone III, $Iz=I(\pi/2,q_0)$ this intensity being constant whatever is the shear rate :

$$I_{iso}(q_0) = I(\omega=\pi/2,q_0) \qquad (5)$$

δ is determined by the adjustment by a Gaussian curve of the variation of the intensity of the Bragg peaks in the $(\vec{z}, \vec{V})$ plan, versus the ω angle (see Fig 7).

To calculate the width Δ of the distribution in the other plane $(\vec{z}, \overrightarrow{\nabla V})$ we replace $I_{iso}(q_0)$ and the expression for the distribution ρ at $\omega=\pi/2$ in the equation 3.

This involves solving the following equation :

$$\overline{I(\omega=\pi/2, q_0)} = \frac{2}{\delta} I_{iso}(q_0) \frac{1}{\Delta} \exp\left(-\pi^2/8\Delta^2\right) \qquad (6)$$

For example, for a lamellar sample $\phi_{26,72}$ the measured width δ is of the order of 20° (see Fig 7) and the ratio $\frac{\overline{I(\omega=\pi/2, q_0)}}{I_{iso}(q_0)}$ is close to 1, the exponential term of equation 6 is also experimentally known. The solution of this equation gives Δ around 45° which corresponds to the mosaicity of the orientation around the axis $\overrightarrow{\nabla V}$ in the $(\vec{z}, \overrightarrow{\nabla V})$ plane.

The resolution function that we can measure on an oriented lamellar phase in a flat capillar [17] is 10% width, that is why we didn't take it into account.

For more dilute samples $\phi_{16,72}$, $\phi_{8,92}$, we found that Δ decreases from about 50° to 35° and saturates at higher shear rates in the region III.

Conclusion

This analysis show us that it is possible to estimate the mosaicity of the orientation in the lamellar phase in all directions. Other experiments like SAXS experiments [17,20] (for which it exists the possibility to send the X-ray beam tangentially to the cell and to probe directly in the $(\vec{z}, \overrightarrow{\nabla V})$ plane) or birefringence measurement (very sensitive to the direction of the normal to the stacked layers), allowed us to find a width of the Gaussian distribution of $\vec{n}$ of the order of 30°

around the $\overrightarrow{vv}$ axis. So the analysis from these last SANS experiments is in agreement with other results, using different techniques.

Obviously, this way of evaluating the degree of the orientation does not reflect the real distribution of defects in the lamellar phase under shear but gives an idea of the quality of this orientation of these lamellar phases at high shear (in the region III of the orientation diagram).

Annex A

The scattered intensity at a $\vec{q}$ from a oriented lamellar phase is proportional to N the number of membranes in the scattering volume, to the form factor of the membrane $P_\perp(q_\perp)$ and $P_{//}(q_{//})$ respectively in the plan and perpendicular to the layers and to the structure factor $S(q_{//})$, the sign '//' meaning the direction normal to the layers. This intensity is calculated as :

$$I(\vec{q}) = N\, P_\perp(\vec{q}_\perp)\, P_{//}(q_{//})\, S(q_{//}) \qquad (A.1)$$

In the space X, Y, Z, the vector normal to these layers $\vec{n}$ is defined by the following angles t and f, and we will suppose that the vector $\vec{q}$ will be located in the plane (Y,Z), defined by the angle ω in this plane (see Fig 6). The components of $\vec{q}$ in function of t, f and ω are the following:

$$q_{//} = \vec{n} \cdot \vec{q} = q \cos\theta = q \sin t \cos(f - \omega) \qquad (A.2)$$

$$q_\perp = q\sqrt{1 - \cos^2\theta} = q\sqrt{1 - \sin t \cos^2(\omega - f)} \qquad (A.3)$$

$\overline{I(q, \omega)}$ is the average intensity for a distribution $\rho(t, f)$ of the vector $\vec{n}$:

$$\overline{I(q,\omega)} = \iint N P_\perp(q\sqrt{1-\alpha^2} P_{//}(q\alpha)\, S(\alpha)\, \rho(t,f)\, dt\, df \qquad (A.4)$$

where $\alpha = \sin(t)\cos(\omega - f)$.

We can assume that $P_\perp(q_\perp)$ which accounts for the finite transverse size of the bilayers can be chosen as a correctly normalized Gaussian function with a maximum $L_\perp^4$ in 0 and with a width $\frac{1}{L_\perp}$(where $L_\perp$ is a correlation length parallel to the layer) which verifies :

$$P_\perp(0) = L_\perp^4 \text{ and } P_\perp(\Delta q) \approx 0 \quad \text{when} \quad \Delta q >> \frac{1}{L_\perp} \qquad (A.5)$$

If we develop f and t around the values which cancel the argument of $P_\perp$,

$$\begin{cases} t = \dfrac{\pi}{2} + \theta \\ f = \omega + \varphi \end{cases} \qquad (A.6)$$

then,

$$P_{\perp}(q\sqrt{1-\alpha^2}) = 2\pi\frac{L_{\perp}^2}{\Delta q^2}\exp\left(-\frac{q_{\perp}^2}{2\Delta q^2}\right) \qquad (A.7)$$

So we can easily resolve the integral over $P_{\perp}$ around $\vec{q_0}$:

$$\int P_{\perp}(q\sqrt{1-\alpha^2})\,dt\,df = 4\pi^2 L_{\perp}^2 \delta(t - \pi/2)\,\delta(f - \omega) \qquad (A.8)$$

Finally for large $q>>\Delta q$ the averaged scattered intensity is calculated as follows:

$$\overline{I(\omega,q)} = 2\pi\frac{NL_{\perp}}{q^2}P_{//}(q)\,S(q)\,\rho(\pi/2,\omega) \qquad (A.9)$$

If we consider the irradiated volume V occupied by N membranes, which is equal to $NdL_{\perp}^2$ the scattered intensity is finally given by :

$$\overline{I(\omega, q)} = \frac{V}{d}\pi\,P(q)\,S(q)\,\rho(\pi/2, \omega) \qquad (A.10)$$

where V is the scattering volume and d the distance between the membranes.

Acknowledgments : I thank the L.L.B for financial support for the 'neutron' Couette cell and also A. Brulet and L. Noirez for their helpful assistance.

References

[1] DIAT O.and ROUX D., *J. Phys. II France* **3** (1993) 9

[2] DIAT O., ROUX D. and NALLET F., submitted to J. Phys. II France

[3] EKWALL P., in Advances in Liquid Crystals (Eds Brown, G.M. Academic, New York, 1975)

[4] TANFORD C.in "the Hydrophobic Effect", (Wiley, New York, 1980, 2nd edition)

[5] ROUX D. and BELLOCQ A-M., *Phys. Rev. Lett.*, **52** (1984) 1895

[6] LARCHE F.C., APPELL J., PORTE G., BASSEREAU P. and MARIGAN J.,*Phys. Rev. Lett.*, **56** (1986) 1700

[7] ROUX D., SAFINYA C.R. and NALLET F., to appear

[8] MEYER R.B., STEBLER B. and LAGERWALL S.T., *Phys. Rev. Lett.*, **41** (1978) 1393

[9] BOLTENHAGEN P., LAVRENTOVICH O. and KLEMAN M., *J. Phys. II France*, **1** (1991) 1233

[10 STREY R., SCHOMAKER R., ROUX D., NALLET F. and OLSSON U., *J. Chem. Soc. Faraday Trans.*, **86** (1990) 2253

[11] NALLET F. and PROST J., *Europhys. Lett.*, **4** (1987) 307

[12] ROUX D. and SAFINYA C.R., *J. Phys. France*, **49** (1988) 307

[13] It is predicted that strong nonlinearities appear at flow rate of order τ_d^{-1} where τ_d is the diffusion time required for the membrane to move in a solvent on a distance of about ξ : for example, for these lamellar phase where this distance is of order of 100 Å we can estimate the shear rate of about 10^6 s^{-1}. In the following experiments the shear rate remains inferior at this value.

[14] SAFINYA C.R., ROUX D., SMITH G.S., SINHA S.K., DIMON P., CLARK N.A. and BELLOCQ A.M., *Phys. Rev. Lett.*, **57** (1986) 2718

[15] This choice of the movement of the two cylinders allows to avoid some hydrodynamic instabilities for Newtonian fluids, at low shear rate

[16] CHANDRASEKHAR S., "Hydrodynamic and Hydromagnetic Instability" (Oxford Press 1968)

[17] DIAT O., thesis n^0833 from University Bordeaux I France (1992)

[18] PORTE G., MARIGNAN J., BASSEREAU P. and MAY R., *Europhys. Lett.*, **7** (1988) 713

[19] LAVERSANNE R., NALLET F. and ROUX D. *J. Phys. II France* **3** (1993) 487

[20] Some SAXS experiment tests have been done at the NSLS on the EXXON X-104 with Safinya C. and collaborators.

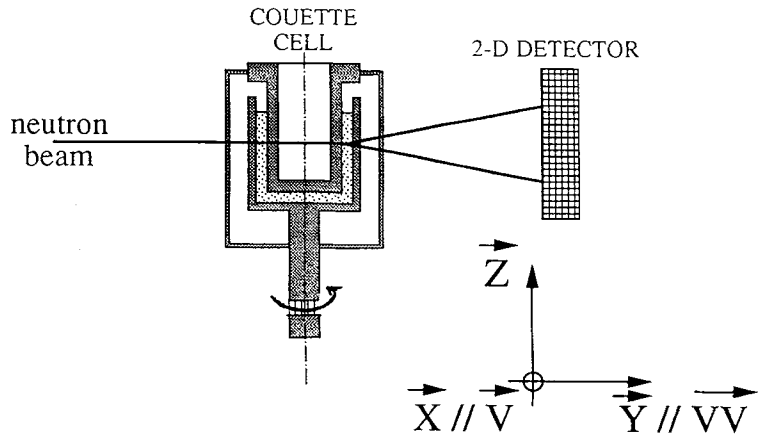

Fig 1 : schematic set-up for SANS measurement on PAXY line with the main axes representation. the neutron beam goes through the cell parallel to the $\overrightarrow{VV}$ axis (which always a radial direction in the Couette geometry).The $\vec{z}$ axis is the vertical and rotation axis for the cylinder. We can choice a gap of .5, 1 or 2 mm and this allow to achieve some shear rates between 0 to 10^5 s^{-1}.

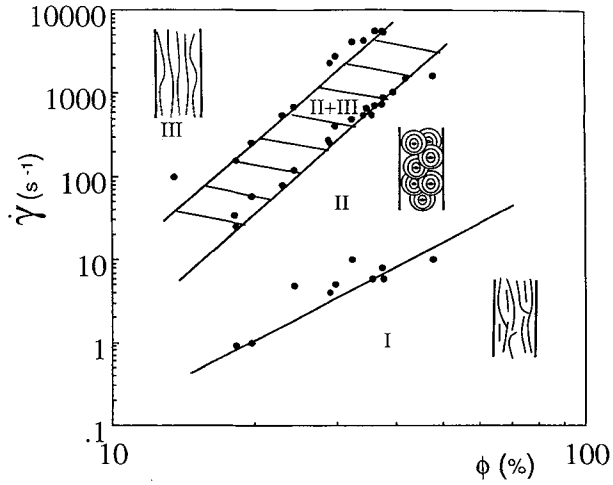

Fig 2 : Orientation diagram where 3 pure orientation states for the lamellar phase are defined where $\dot{\gamma}$ is the shear rate and ϕ the volume fraction of membrane. The straight line represent the limits between these different zones. The first one (region I) corresponds to a state for which the lamellar phase is oriented with the membranes parallel to the surface of the cylinders, with a lot of defects moving in the flow. The second one corresponds to a liquid of close contact spherulites. There are some spherical multilayer vesicles which can roll over each other in the flow. Region III corresponds to the same orientation as for region I but with no more defects in the flow direction and so to a better oriented lamellar phase. The crossed region called II+III correspond to a coexistence zone with two orientation II and III which is spatially alternated in the annular gap.

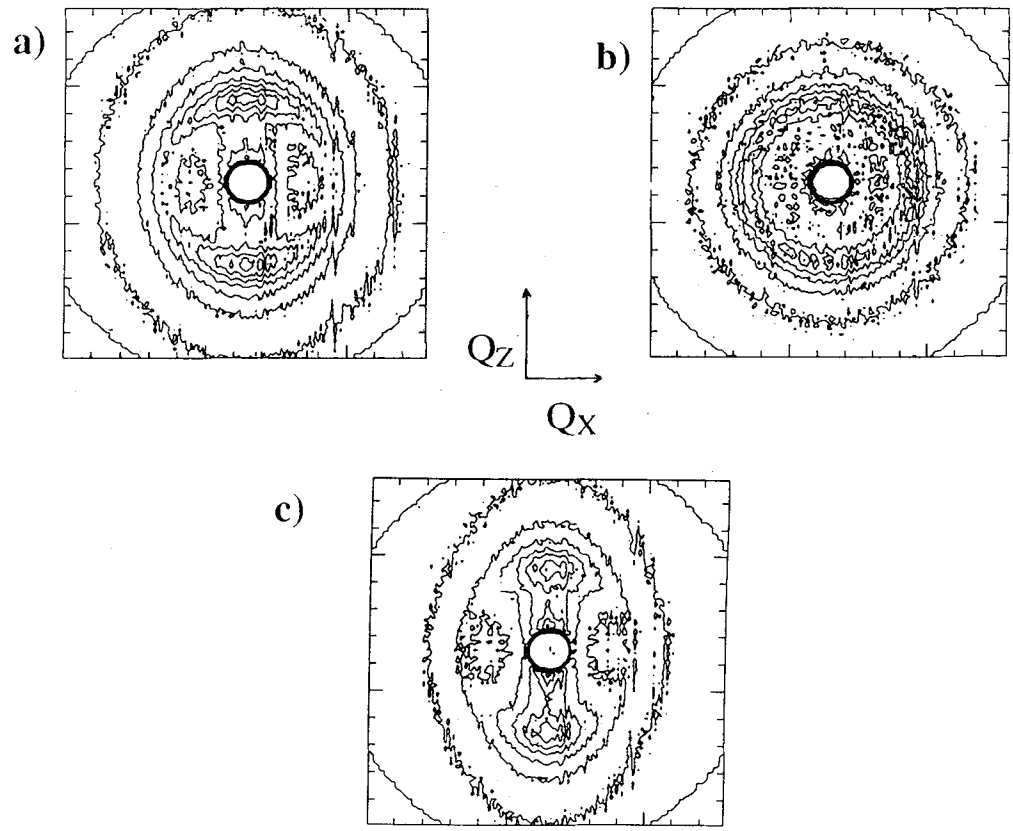

Fig 3 : evolution of the 2 dimensional scattering pattern from a lamellar phase $\phi_{37.44}$ under shear measured in every three region defined previously in the orientation diagram (a/ $\dot{\gamma}$ =1s^{-1} b/ $\dot{\gamma}$ =14s^{-1} ; c/ $\dot{\gamma}$ =3467 s^{-1})

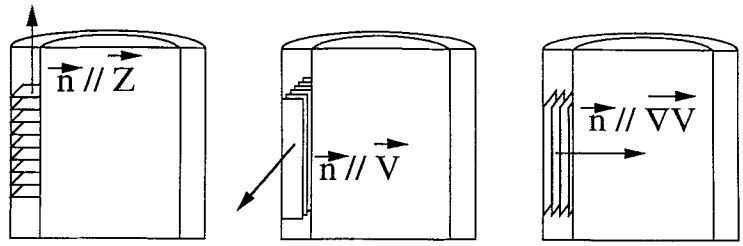

Fig 4 : schematic representation of the three pure orientations of the lamellae in the Couette cell. We call the orientation by the direction of $\vec{n}$ the normal to the layers ; for example the main orientation in the region III correspond to the third representation , the orientation gradV (radial orientation).

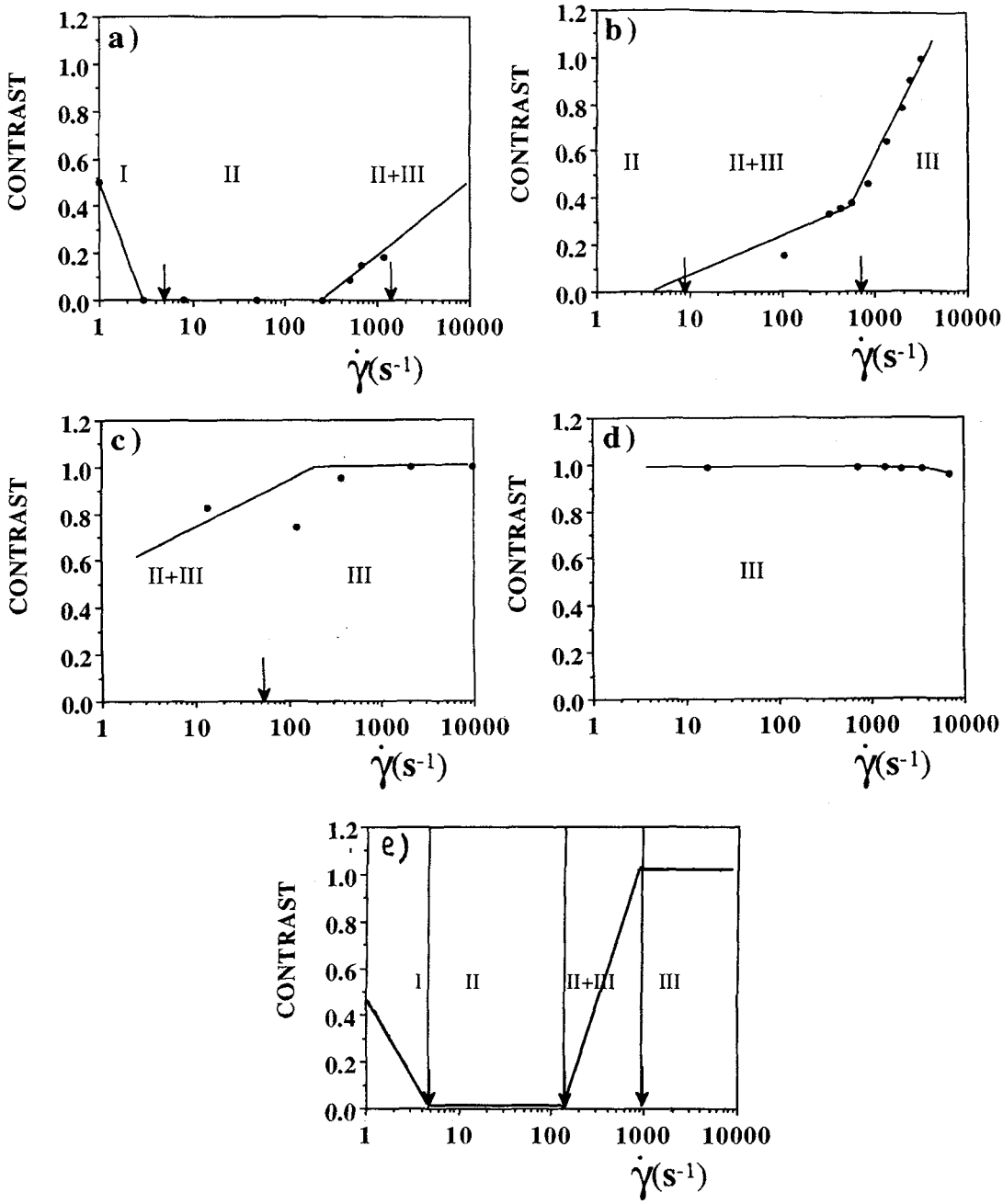

Fig5 : variation of the contrast versus the shear rate for different membrane concentrations (a/ $\phi_{46.6}$, b/ $\phi_{27.2}$, c/ $\phi_{16.72}$, d/ $\phi_{8.92}$,.e/ generic curve). The straight lines on every graph are only some guides to follow the variation of the contrast while the shear rate increases. The arrows allow us to distinguish the limits of the different regions of the orientation diagram.

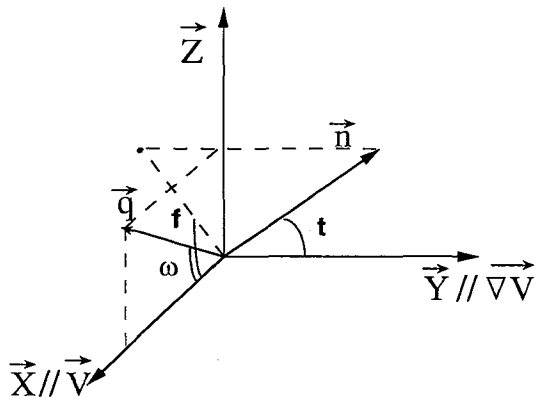

Fig 6 : definition of the different angles used for the analysis.

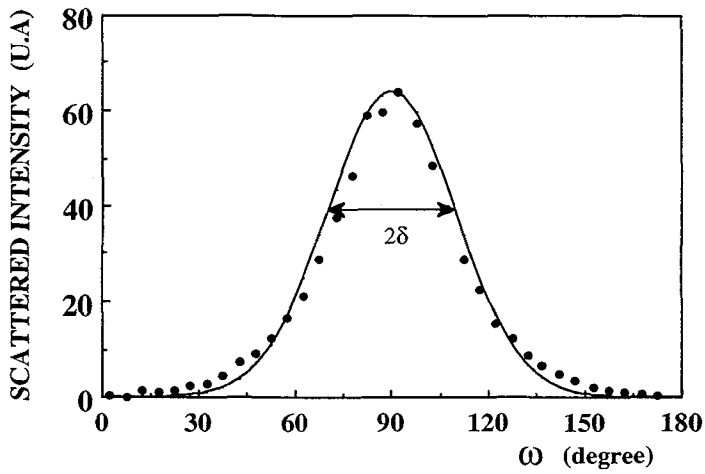

Fig 7 : variation of the Bragg intensity versus ω angle in the plan of the detector for the lamellar phase $\phi_{27.2}$ at high shear rate (region III). The maximum of the data corresponds to the intensity of the Bragg peak in the Z direction. The curve corresponds to a Gaussian fit which allows us to determine δ and then to resolve the equation 6.